Rheological properties of a reentrant nematic liquid crystal

J. Ananthaiah,[1] M. Rajeswari,[1] V. S. S. Sastry,[1] R. Dabrowski,[2] and Surajit Dhara[1,*]
[1]*School of Physics, University of Hyderabad, Hyderabad 500046, India*
[2]*Institute of Chemistry, Military University of Technology, 00-908 Warsaw, Poland*
(Received 20 February 2012; revised manuscript received 2 June 2012; published 25 July 2012)

We report experimental studies on small angle light scattering (SALS), and rheodielectric and electrorheological properties of a binary mixture of octyloxy cyanobiphenyl and hexyloxy cyanobiphenyl liquid crystals. The mixture exhibits nematic (N) to smectic-A (SmA) phase transitions, and then again to a reentrant nematic (N_R) phase transition. Rapid shear thinning in the quenched samples in the low shear rate region in the N and SmA phases observed from SALS experiments is attributed to the realignment of the director within the domains. The domains are elongated along the shear direction at higher shear rates. The temperature variation of the effective viscosity and static dielectric constant reveals the changes in the director orientation across N-SmA-N_R phase transitions. At a steady shear rate the effective viscosity increases with the electric field in all the phases and saturates at much higher fields. It also exhibits two anomalous peaks across N-SmA-N_R phase transitions beyond a particular field. The shear modulus of the SmA phase in an intermediate field is significantly larger than that measured at both low and high fields. This enhanced viscoelasticity of the SmA phase is argued to originate from the increased dislocation density.

DOI: 10.1103/PhysRevE.86.011710 PACS number(s): 83.80.Xz, 83.10.Tv, 83.50.Ax

I. INTRODUCTION

Liquid crystals are orientationally ordered fluids made of anisotropic organic molecules. They exhibit a variety of phase transitions owing to their molecular structures and shapes. Common mesophases exhibited by low molecular weight liquid crystals (LCs) are typically nematic (N), smectic-A (SmA) and cholesteric (N^*). The flow properties of these LCs are very interesting and there are many theoretical and experimental studies on the flow viscosities [1–14]. Nematic liquid crystals (NLCs) in this respect are relatively simpler and have been investigated in detail [3]. The average alignment direction of the long axes of the molecules is called the director and is denoted by a dimensionless unit vector **n**. When the sample is sheared the director exhibits mainly three types of orientation with respect to the flow and the velocity gradient directions. Schematic representations of the director orientations in N as well as in SmA phases are shown in Fig. 1. The orientation of the director depends on the relative magnitude and sign of the two Leslie coefficients, α_2 and α_3. If both of these coefficients are negative the director aligns at an angle $\theta = \tan^{-1}(\sqrt{\alpha_2/\alpha_3})$ with respect to the flow direction [4,15–17]. In this orientation the measured viscosity is η_2 (Miesowicz viscosity). Safinya *et al.* [13] reported that the director orientation changes with temperature in compounds exhibiting N-SmA phase transition. They showed theoretically and experimentally that α_3 is renormalized ($\alpha_3^R > 0$) due to the critical slowing down of the SmA order-parameter fluctuations in the N phase, and the ratio α_2/α_3 is negative [13,14]. As a result the director orientation changes from the flow direction to a neutral direction (x axis) as shown in Fig. 1(a). Later it was shown that in the case of freely flowing nematic liquid crystals the measured viscosity changes from η_2 to η_3 at a few degrees below the nematic-isotropic (NI) transition [18,19]. It suggests that just below the NI transition the director is oriented along the velocity direction (Fig. 1(b)) and changes its orientation to the neutral direction (as shown in Fig. 1(a)) as the temperature is reduced. Bhattacharya *et al.* measured flow viscosity in an oriented sample showing SmA-to-N_R phase transition [20] and reported that the flow behavior of the N_R phase is identical to that of the higher temperature nematic phase.

Using synchrotron x-ray studies Safinya *et al.* [14] showed that several steady state structures appear in compounds exhibiting N-SmA transition due to the precessional motion of the director along the neutral direction [14] denoted by a_m, a_s, $a(b)$, and a_c. These structures are described by the equation of an ellipse: $n_y^2(t)/n_{y0}^2 + n_z^2(t)/n_{z0}^2 = 1$, where $n_y(t) = n_{y0}\cos(\omega_0 t)$ and $n_z(t) = n_{z0}\sin(\omega_0 t)$ are components of the director $\mathbf{n}(t) = (n_x(t), n_y(t), n_z(t))$. The angular frequency of the precessional motion is given by $\omega_0 = \sqrt{\dot{\gamma}^2(-\alpha_2\alpha_3^R)/\gamma_1^2}$, where α_3^R is the renormalized Leslie coefficient, $\dot{\gamma}$ is the shear rate, and $\gamma_1 = \alpha_3 - \alpha_2$ [14]. These structures are physically interpreted as follows. In a_m structure, the precessional motion is anisotropic with larger amplitude in the y direction than in the z direction ($n_{y0} > n_{z0}$); in a_s structure, the isotropic precession occurs with equal amplitudes in both directions ($n_{y0} = n_{z0}$); in $a(b)$ structure, anisotropic precession occurs with lesser amplitude in the y direction than in the z direction ($n_{y0} < n_{z0}$); and in a_c structure, anisotropic precession occurs with a very large amplitude in the z direction ($n_{y0} \ll n_{z0}$). Negita *et al.* [21] reported that the above structural features are also reflected in the rheodielectric measurements on octyl cyanobiphenyl (8CB) compound which exhibits N-SmA phase transition. Very recently we showed that the viscosity increases and the director orientation changes under the application of an external electric field when the temperature is reduced in octyloxy cyanobiphenyl (8OCB) [22]. The rheodielectric measurements mostly provide overall information on the director orientation during the flow. However, small angle light scattering (SALS) measurements have the potential to infer the effect of domain shape and size on the rheological properties and such studies are meager in these materials. In addition, the flow behavior and hence the rheological

*Corresponding author: sdsp@uohyd.ernet.in

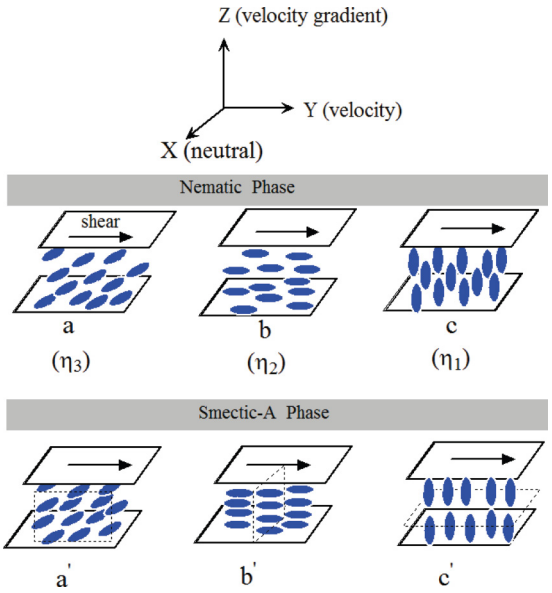

FIG. 1. (Color online) Schematic representation of the three fundamental director orientations in the N and SmA phases under shear. The director orientations are along the x (neutral), y (velocity), and z (velocity gradient) directions, denoted a, b, and c, respectively. Similar director orientation in the SmA phase is denoted by a', b', and c'. Layer orientations in the SmA phase are shown by dotted lines. Miesowicz viscosities corresponding to each orientation in the N phase are designated by η_3, η_2, and η_1, respectively.

properties across the SmA-to-N_R transition are very rare and interesting from a phase transition point of view.

In this paper we report SALS, rheodielectric, and electrorheological studies on a binary mixture of hexyloxy cyanobiphenyl (6OCB) and 8OCB and investigate the effect of an external ac electric field on the effective viscoelastic properties. We emphasize that the flow behavior and effect of presmectic fluctuations are similar in both N and N_R phases. The viscoelasticity in the SmA phase is dominated by dislocations and shows an interesting variation on the application of an external field.

II. EXPERIMENT

The compounds 8OCB and 6OCB were synthesized in our laboratory in Poland. 6OCB exhibits only the N phase, while 8OCB exhibits both N and SmA phases. A 6OCB with 8OCB mixture of 21.0 to 29.5 wt% exhibits the reentrant nematic (N_R) phase. There have been several studies on the phase transitions in these mixtures [23,24]. We have chosen a mixture of 27 wt% of 6OCB and 73 wt% of 8OCB that exhibits a reasonably wide temperature range ($\simeq$10°C) of the SmA phase above the reentrant nematic phase. The mixture shows the following phase sequence as observed in a polarizing optical microscope on cooling: N_R 32.4°C; SmA 43.2°C; N 77.5°C I. Rheological measurements were performed using a rheometer (Anton Paar MCR 501) in parallel plate geometry with a plate diameter of 50 mm. The parallel plate configuration was chosen for the simultaneous measurement of rheological and dielectric properties. The gap between the two parallel plates was 75 μm.

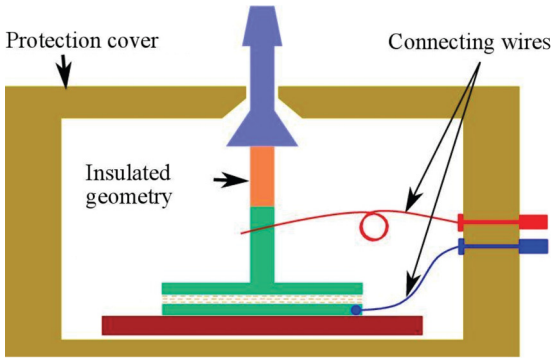

FIG. 2. (Color online) Schematic representation of the parallel plate setup for simultaneous measurement of rheological and dielectric properties.

The schematic diagram for measuring the rheodielectric properties is shown in Fig. 2. An electric field was applied between the bottom and the top plates by using a low friction spring wire (Fig. 2). The *air correction* (i.e., the contribution due to the small friction in the absence of the sample) was estimated. These values were subtracted from the measured quantities in the presence of the sample at all temperatures and electric fields. The temperature variation of the dielectric constant was measured by measuring the ratio of the sample capacitance with that of the capacitance of an empty cell (i.e., without sample). The temperature of the sample was controlled by a Peltier temperature controller with an accuracy less than 0.1°C. The heater and the measuring system were kept inside a protective cover for uniformity of the sample temperature. The dielectric constant was measured as a function of temperature up to 20 V with an inductance-capacitance-resistance (LCR) meter (Agilent E4980A). For voltages beyond 20 V we used a signal generator (Tektronix AFG3102) and a high voltage amplifier (TEGAM). The frequency of the sinusoidal voltage was 3.11 kHz for all the measurements. The experimental setup for SALS is shown in Fig. 3, and parallel glass plates of diameter 43 mm were used in these measurements. The upper limit of temperature of the SALS experiment is 70°C. A polarized diode laser of wavelength 658 nm was directed to the sample. An analyzer crossed with respect to the polarizer, a beam stopper, and a focusing lens were adjusted to obtain the scattering pattern on the screen. A CCD camera was used to record the scattering pattern. Samples were prepared by physical mixing without any solvent and all the measurements were made upon cooling the sample from the isotropic phase.

III. RESULTS AND DISCUSSION

A. SALS measurements

We first present the variation of effective shear viscosity (η_{ef}) in a *quenched* sample with shear rate, in both N and SmA phases (Fig. 4). In the N phase η_{ef} is very high ($\simeq$700 mPa s) in the low shear rate region (e.g., $\dot{\gamma} = 0.1\ s^{-1}$) and exhibits strong shear thinning behavior. For example, it reduces to $\simeq$35 mPa s at $\dot{\gamma} \simeq 10\ s^{-1}$. Beyond this shear rate η_{ef} is constant and hence behaves like a Newtonian fluid. The shear rate dependent effective viscosity in the N phase can be described using the

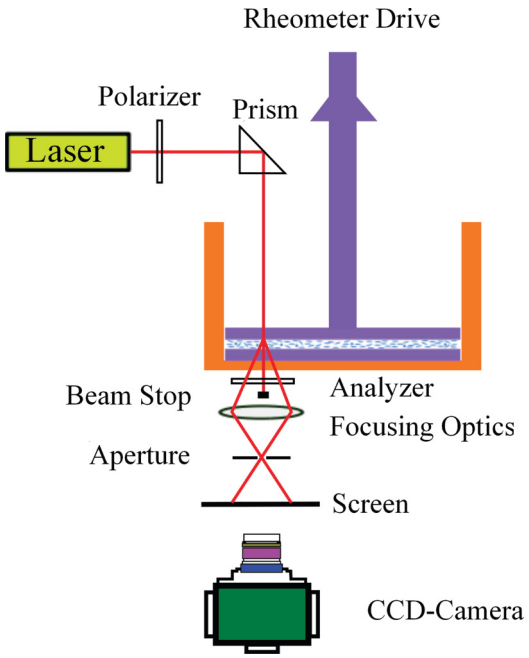

FIG. 3. (Color online) Schematic representation of small angle light scattering (SALS) setup with the rheometer.

Sisco model [25]

$$\eta = \eta_\infty + a\dot{\gamma}^{-n}, \tag{1}$$

where η_∞ and n are the asymptotic value of the viscosity (at very high shear rate) and the power-law index, respectively. The best fit to the Sisco model is shown in Fig. 4. The index n is about 0.8 and comparable to the previously reported value [26]. In the SmA phase η_{ef} is about ten times higher than in the N phase and exhibits shear thinning behavior up to $\dot{\gamma} = 50\ s^{-1}$. At higher shear rate η_{ef} does not saturate, indicating the presence of multiple shear thinning events.

The depolarized scattering patterns obtained from the horizontal-vertical orientation of the polarizers (HV) at some representative shear rates are also shown in Fig. 4, and the shape remains symmetric (almost circular) up to $\dot{\gamma} = 10\ s^{-1}$ in the N phase. Beyond this shear rate the shape is elongated normal to the shear direction and tends to be elliptical. Nematic liquid crystals normally exhibit a polydomain texture, separated by spatially distributed disclination lines. Since SALS measures the image in the **q** space, it suggests that, below $\dot{\gamma} = 10\ s^{-1}$, the reorientation of the director takes place such that it tends to orient parallel to the shear plane without affecting the domain shape. At higher shear rate the polydomain texture is elongated along the shear direction. In the SmA phase a non-Newtonian flow behavior is observed in the entire range of shear rate, and beyond $\dot{\gamma} = 50\ s^{-1}$ the onset of elongation of the scattering pattern is observed. Thus, this threshold shear rate is almost five times larger than that of the N phase. The SmA phase has focal conic domains with spatially distributed dislocations in the sample. The realignment of the director, and hence the SmA layers, take place within $\dot{\gamma} = 50\ s^{-1}$. The elongation of domains occurs beyond this shear rate. This was also observed previously in a polarizing optical microscope [27] but the shear rate dependent shape was not reported. It may be mentioned that the scattering intensity also increases with shear rate in both phases and similar behavior was also observed in other systems [28,29]. Since HV scattering in the present sample arises preliminarily from orientational fluctuations, it suggests that these fluctuations are increasing with shear rate.

We measured the temperature dependent effective viscosity (η_{ef}) at a steady shear rate ($\dot{\gamma} = 50\ s^{-1}$) and recorded the scattering patterns at some representative temperatures to investigate the domain structure. It was not possible to record SALS patterns above $T - T_{NI} \simeq -15°C$ due to the limitations of the associated temperature controller. In Fig. 5 we present the variation of η_{ef} with temperature and a few SALS patterns. We find that η_{ef} decreases in the N phase just below the NI transition. This is due to the shear-induced alignment of the director along the shear direction as shown in Fig. 1(b). Below $T - T_{NI} = -4°C$, η_{ef} begins to increase, suggesting the

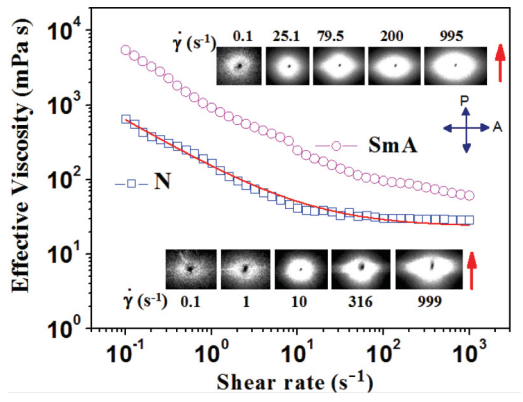

FIG. 4. (Color online) Shear rate dependent effective shear viscosity (η_{ef}) in N ($T - T_{NI} = -30°C$) and SmA phases ($T - T_{NI} = -43°C$). The depolarized scattering patterns (HV) at some representative shear rates are shown in both the phases. The red arrow indicates the direction of shear. The upper and lower scattering patterns correspond to the SmA and N phases, respectively. The continuous line is a best fit to Eq. (1).

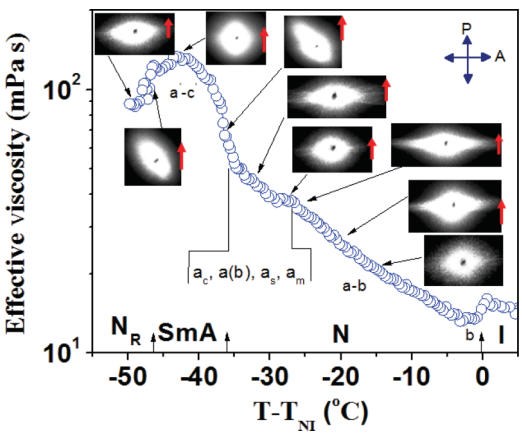

FIG. 5. (Color online) Temperature variation of effective shear viscosity (η_{ef}) at a steady shear rate ($\dot{\gamma} = 50\ s^{-1}$). HV scattering patterns at a few temperatures. The red arrow indicates the direction of shear. The possible director orientations at different temperatures are also indicated considering the similarity of temperature dependent zero-field viscosity of 8CB [21] and 8OCB [22].

onset of a mixed director orientation (i.e., *a*-*b* structure). The viscosity increases almost linearly up to $T - T_{NI} \simeq -25^{\circ}$C. A small slope change below this temperature, followed by a rapid increase of the viscosity in the Sm*A* phase, is observed. Similar behavior of η_{ef} was also observed above the *N*-Sm*A* phase transition in pure 8CB and 8OCB liquid crystals [21,22]. It was explained based on the occurrence of various structures, namely a_c, $a(b)$, a_s, and a_m, that arise because of precessional motion of the director, discussed earlier. The scattering patterns at this shear rate ($\dot{\gamma} = 50\ s^{-1}$) in the *N* phase (Fig. 5) are elongated perpendicular to the shear direction due to the deformation of domains, as explained previously. The orientation of the patterns at *N*-Sm*A* and Sm*A*-N_R transitions is noticeably different in the sense that the long axis of the ellipse is rotated by an angle $\simeq 45^{\circ}$ to the left side of the shear direction. This implies that the elongation directions of the domains are rotated by the same angle on the right side of the shear direction. It seems that the precessional motion of the director (as described by Safinya *et al.* [14]) also induces significant change in the microtexture of the sample. In the Sm*A* phase the domains have c' and a' director orientation (Fig. 1), and the scattering pattern is almost circular (Fig. 5), suggesting that the shapes of the domains remain unaffected at this shear rate. This is also consistent with the observation in Fig. 4. In the N_R phase the viscosity decreases sharply and again the scattering pattern gets elongated perpendicular to the shear direction.

B. Rheodielectric and electrorheological measurements

To investigate the director orientation inside the domain we measured the effective dielectric constant (ϵ_{ef}) simultaneously with the viscosity measurement as a function of temperature at various fields. First we show the electric field-dependent effective viscosity (η_{ef}) as a function of temperature in Fig. 6(a). Its behavior at a low field (i.e., 0.8×10^4 V/m) was already discussed in Fig. 5 and is presented here again for the purpose of comparison with the data at higher field. At a fixed temperature in the *N* phase, η_{ef} increases with electric field and saturates beyond a threshold value (26.7×10^4 V/m). It exhibits two anomalous peaks [Fig. 6(a)] across *N*-Sm*A*-N_R phase transitions beyond a particular field ($>13.3 \times 10^4$ V/m). At much higher field the peaks become sharper and they tend to get suppressed beyond $\simeq 93.3 \times 10^4$ V/m [Fig. 6(a), inset]. The anomalous behavior of η_{ef} across the *N*-Sm*A* transition was also observed in a few liquid crystals and it was attributed to the significant contribution of the Leslie coefficient α_1 near the *N*-Sm*A* transition [10,30]. Since the hydrodynamic theory of both the *N* and N_R phases is expected to be the same [20], the second peak across the Sm*A*-N_R transition could be due to the similar effect. Furthermore, it may be noted that both the peaks are asymmetric in shape with temperature and the second peak is relatively stronger than the first one. The origin of this asymmetry in not clear, however; the difference in the smectic short-range order in both *N* and N_R phases could be responsible.

The variation of ϵ_{ef} that was measured simultaneously with the viscosity measurement is shown in Fig. 6(b). At *zero* shear rate and low field (0.8×10^4 V/m) in the *N* phase, ϵ_{ef} is lower than in the I phase, suggesting that the parallel plate

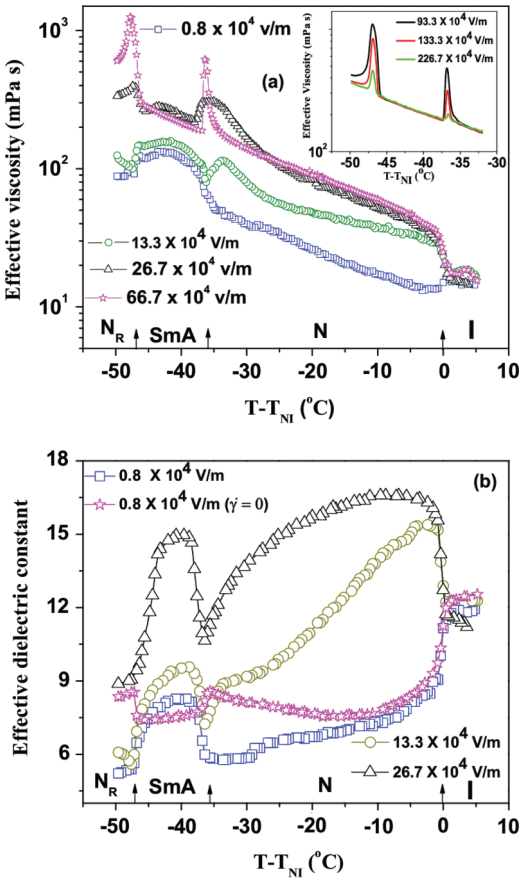

FIG. 6. (Color online) (a) Variation of effective shear viscosity (η_{ef}) with temperature at various ac electric fields. All the data were collected at a steady shear rate ($\dot{\gamma} = 50\ s^{-1}$). Inset: Suppression of peaks under strong electric fields. (b) Static dielectric constant at same shear rates and same electric fields as in (a). The dielectric data represented by star were measured without shear and at a field 0.8×10^4 V/m. The frequency of the applied field is 3.11 kHz.

induces planar orientation of the director. Since the dielectric anisotropy ($\Delta\epsilon = \epsilon_{||} - \epsilon_{\perp}$) of the mixture is positive [31] we essentially measure the perpendicular component, i.e., $\epsilon_{ef} \simeq \epsilon_{\perp}$. In the Sm*A* phase ϵ_{ef} is comparatively lower than both the *N* and the N_R phases, indicating a strong antiparallel correlation of the transverse component of the dipole moments in the Sm*A* layers [32]. At the same field the temperature variation of ϵ_{ef} is significantly different when the sample is subjected to a steady shear rate ($\dot{\gamma} = 50\ s^{-1}$), especially below $T - T_{NI} = -10^{\circ}$C. This is because of the orientational change of the director across the phase transitions. In the Sm*A* phase ϵ_{ef} is slightly larger than the values in both *N* and N_R phases due to the a'-c' orientation of Sm*A* layers as described in Fig. 5. At an intermediate field (e.g., 13.3×10^4 V/m), ϵ_{ef} just below the NI transition is much larger than in the I phase and decreases gradually with decreasing temperature. Initially the director tends to orient along the field direction as $\Delta\epsilon > 0$. On the other hand, due to the effect of shear and presmectic fluctuations it tends to be parallel to the shear plane with decreasing temperature. Thus, at every temperature the direction of director orientation is determined by these two competing force fields. When the electric field is increased

to 26.7×10^4 V/m, ϵ_{ef} is much higher and $\epsilon_{ef} \simeq \epsilon_{||}$ [33] and decreases gradually as the N-SmA transition is approached. In the SmA phase ϵ_{ef} again increases and reaches a maximum value ($\epsilon_{ef} \simeq 15$) which is slightly less than that measured in the N phase (near the NI transition), suggesting that the layer orientation in this phase is almost c′ type.

C. Field-dependent complex shear modulus measurements

The experimental results from the SALS measurement provided qualitative information about the microtexture, and the rheodielectric properties revealed the changes in the director orientation. In the phase diagram of this binary mixture the SmA phase is surrounded by the nematic phase [23] and has different types of defects (dislocations). We anticipated that the investigation on the shear modulus across the phase transitions could be interesting in the sense that the applied electric field can change the defect density. Hence we measured the storage and loss moduli (G' and G'') as a function of temperature. In Fig. 7 we show the variation of G' and G'' as a function of temperature at various applied electric fields. At a low field (0.8×10^4 V/m) G' and G'' are very small ($\simeq$0.5 Pa) in both N and N_R phases compared to the SmA phase ($\simeq$20 Pa). Both G' and G'' increase in the SmA phase when the field is increased to 13.3×10^4 V/m and decrease again at much higher field (66.6×10^4 V/m). For example, in the middle

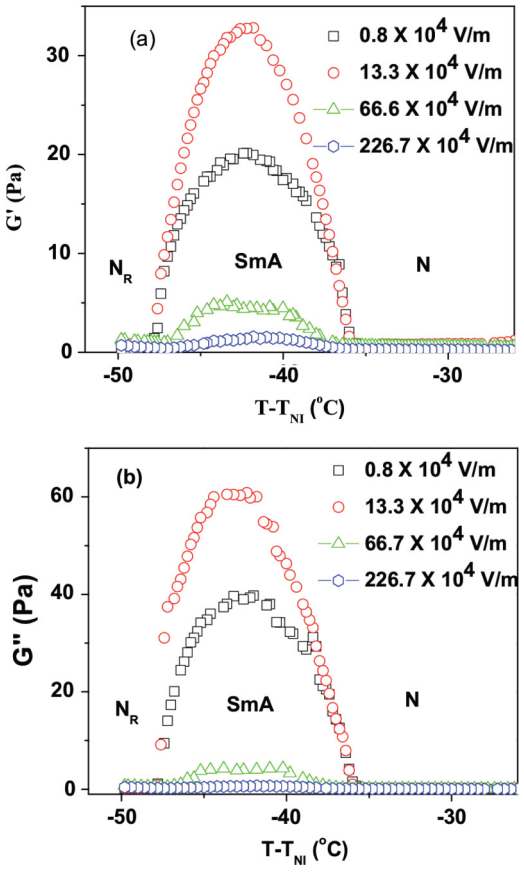

FIG. 7. (Color online) Variation of (a) storage modulus (G') and (b) loss modulus (G'') across N-SmA-N_R phase transitions at various ac electric fields at an angular frequency $\omega = 10$ rad/s and strain amplitude $\gamma = 0.05$.

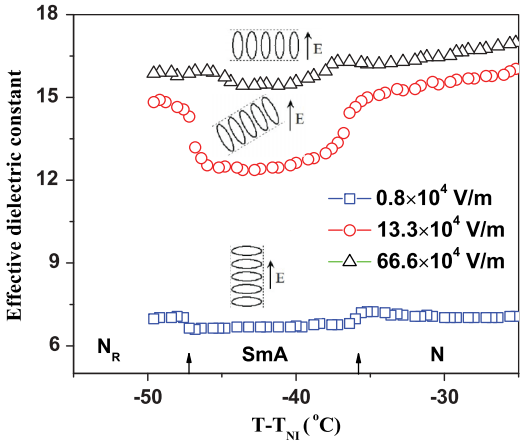

FIG. 8. (Color online) Variation of effective dielectric constant (ϵ_{ef}) across N-SmA-N_R phase transitions at various ac electric fields at an angular frequency $\omega = 10$ rad/s and strain amplitude $\gamma = 0.05$. The frequency of the applied field is 3.11 kHz. Orientations of SmA layers with respect to field direction are shown schematically.

of the SmA phase (i.e., $T - T_{NI} = -42°$C) at a low field (0.8×10^4 V/m), $G' \simeq 20$ Pa and increases to $\simeq$32 Pa at a field 13.3×10^4 V/m and then decreases to a small value $\simeq$4 Pa beyond 226.7×10^4 V/m. Similar behavior with temperature and field is also observed in the case of G''.

To understand the temperature variation of G' and G'' at various fields we simultaneously measured the effective dielectric constant (ϵ_{ef}) as a function of temperature as shown in Fig. 8. It is noticed that ϵ_{ef} at low field (0.8×10^4 V/m) in N, SmA, and N_R phases are comparable to the perpendicular component of the dielectric constant ($\epsilon_\perp$) measured in a surface aligned planar cell [33], suggesting that the SmA layers within the domains are oriented parallel to the field direction as shown in Fig. 8. When the field is increased to 13.3×10^4 V/m, ϵ_{ef} increases in all the phases due to the partial alignment of the director along the field direction. However, at the same field ϵ_{ef} is comparatively lower in the SmA phase than in both the N and N_R phases. For example, at the middle of the SmA temperature range (i.e., $T - T_{NI} = -42°$C) $\epsilon_{ef} \simeq 12.5$ whereas in both N and N_R phases it is $\simeq$15. At much higher field (66.7×10^4 V/m) ϵ_{ef} is almost comparable in all the phases, indicating that the director, and hence the layer normal, is almost parallel to the field direction. This suggests that in the intermediate field (13.3×10^4 V/m) SmA layers (within the domains) are oriented such that the layer normals in different domains are tilted in different directions with respect to the field direction. Such orientations of SmA layers are expected to create more dislocations, and as a result both the shear moduli can increase (in Fig. 7). At high field (66.7×10^4 V/m) the dislocation density decreases due to the almost complete orientation of the SmA layers (Fig. 8) and both the moduli decrease.

IV. CONCLUSIONS

In conclusion, we have shown that strong shear thinning is due to both the elongation of domains and the realignment of a director within the domains in both N and SmA phases. The domain elongation starts beyond a threshold shear rate and in the case of SmA this shear rate is about five times higher

than in the N phase. The director orientation changes under the application of electric field as the temperature is reduced across N-SmA-N_R phase transitions. We presented possible layer orientations at various electric fields and showed that the zero-field viscoelasticity in the SmA phase is aided by the presence of dislocations, which disappear on application of strong external field.

ACKNOWLEDGMENTS

S.D. gratefully acknowledges financial support from DST, Government of India (Grant No. SR/NM/NS-134/2010) and CSIR (Grant No. 03(1207)/12/EMR-II). J.A., M.R., and S.D. gratefully acknowledge the support from UGC-CAS, School of Physics.

[1] P. G. de Gennes, *The Physics of Liquid Crystals*, 2nd ed. (Oxford University Press, Oxford, 1993).

[2] S. Chandrasekhar, *Liquid Crystals*, 2nd ed. (Cambridge University Press, Cambridge, 1992).

[3] V. V. Belyaev, *Viscosity of Nematic Liquid Crystals*, 1st Indian ed. (Cambridge International Science Publishing, Cambridge, 2011).

[4] F. M. Leslie, J. Mech. Appl. Math. **19**, 357 (1966).

[5] M. Miesowicz, Nature (London) **17**, 261 (1935).

[6] M. Miesowicz, Bull. Acad. Pol. Sci. A **28**, 228 (1936).

[7] Ch. Gahwiller, Phys. Lett. A **36**, 311 (1971).

[8] Ch. Gahwiller, Mol. Cryst. Liq. Cryst. **20**, 301 (1973).

[9] H. Kneppe, F. Schneirder, and N. K. Sharma, J. Chem. Phys. **77**, 3203 (1982).

[10] K. Negita, Int. J. Mod. Phys. B **13**, 2005 (1999).

[11] K. Negita, J. Chem. Phys. **105**, 7837 (1996).

[12] Orsay Liquid Crystal Group, Mol. Cryst. Liq. Cryst. **13**, 187 (1971).

[13] R. F. Bruinsma and C. R. Safinya, Phys. Rev. A **43**, 5377 (1991).

[14] C. R. Safinya, E. B. Sirota, and R. J. Plano, Phys. Rev. Lett. **66**, 1986 (1991).

[15] J. L. Ericksen, Arch. Ration. Mech. Anal. **4**, 231 (1960).

[16] T. Carlsson and K. Skarp, Mol. Cryst. Liq. Cryst. **78**, 157 (1981).

[17] T. Carlsson and K. Skarp, Mol. Cryst. Liq. Cryst. **104**, 307 (1984).

[18] J. Jadzyn and G. Czechowski, J. Phys.: Condens. Matter **13**, L261 (2001).

[19] J. Jadzyn and G. Czechowski, Phys. Rev. E **64**, 052702 (2001).

[20] S. Bhattacharya and S. V. Letcher, Phys. Rev. Lett. **44**, 414 (1980).

[21] K. Negita, M. Inoue, and S. Kondo, Phys. Rev. E **74**, 051708 (2006).

[22] J. Ananthaiah, M. Rajeswari, V. S. S. Sastry, R. Dabrowski, and S. Dhara, Eur. Phys. J. E **34**, 74 (2011).

[23] P. E. Cladis, D. Guillon, F. R. Bouchet, and P. L. Finn, Phys. Rev. A **23**, 2594 (1981).

[24] A. R. Kortan, H. V. Kanel, R. J. Birgeneau, and J. D. Litster, Phys. Rev. Lett. **47**, 1206 (1981).

[25] H. A. Barnes, J. F. Hutton, and K. Walters, *An Introduction to Rheology* (Elsevier, Amsterdam, 1989).

[26] M. T. Cidade, G. Pereira, A. Bubnov, V. Hamplova, M. Kaspar, and J. P. Casquilho, Liq. Cryst. **39**, 191 (2012).

[27] S. Fujii, S. Komura, Y. Ishii, and C. Y. D. Lu, J. Phys.: Condens. Matter **23**, 235105 (2011).

[28] B. Hsiao, R. S. Stein, and K. Deutscher, J. Polym. Sci., Part B: Polym. Phys. **28**, 1571 (1990).

[29] B. Schubert, N. J. Wagner, and E. W. Kaler, Langmuir **20**, 3564 (2004).

[30] K. Negita, Mol. Cryst. Liq. Cryst. **300**, 163 (1997).

[31] A. Kubono, K. Yoshino, T. Ninomiya, R. Akiyama, and K. Tanaka, Liq. Cryst. **29**, 1089 (2002).

[32] W. H. de Jeu, *Physical Properties of Liquid Crystal Materials* (Gordon and Breach, New York, 1980).

[33] We measured parallel ($\epsilon_{||}$) and perpendicular ($\epsilon_{\perp}$) components of the dielectric constant in planar and homeotropic cells as a function of temperature. We found $\epsilon_{\perp} \simeq 5.9$ and $\epsilon_{||} \simeq 16.5$ at $T - T_{NI} = -45^{\circ}$C. The subscripts refer to directions in relation to the director.